Enhanced self-field critical current density of nano-composite $YBa_2Cu_3O_7$ thin films grown by pulsed-laser deposition

(*Short title*: Enhanced critical current density of nano-composite $YBa_2Cu_3O_7$ thin films)

K. Siraj, J.D. Pedarnig *, A. Moser, D. Bäuerle
Institut für Angewandte Physik, Johannes-Kepler-Universität Linz, A-4040 Linz, Austria

N. Hari Babu, D.A. Cardwell
Department of Engineering and IRC in Superconductivity, University of Cambridge,
Trumpington Street, Cambridge, CB2 1PZ, UK

PACS: 74.78.Bz High-T_c films
81.15.Fg Laser deposition
68.55.Nq Composition and phase identification

Abstract

Enhanced self-field critical current density J_c of novel, high-temperature superconducting thin films is reported. Layers are deposited on (001) MgO substrates by laser ablation of $YBa_2Cu_3O_{7-\delta}$ (Y-123) ceramics containing $Y_2Ba_4CuMO_x$ (M-2411, M = Ag, Nb, Ru, Zr) nano-particles. The J_c of films depends on the secondary phase content of the ceramic targets, which was varied between 0 and 15 mol %. Composite layers (2 mol % of Ag-2411 and Nb-2411) exhibit J_c values at 77 K of up to 5.1 MA/cm^2, which is 3 to 4 times higher than those observed in films deposited from phase pure Y-123 ceramics. Nb-2411 grows epitaxially in the composite layers and the estimated crystallite size is ~ 10 nm.

* corresponding author: Johannes.Pedarnig@jku.at

The critical current density J_c of high-temperature superconducting $YBa_2Cu_3O_7$ (Y-123) epitaxial thin films is, typically, in the range of 10^6 to 10^7 A/cm^2 at temperatures T ≤ 77 K in self-field, i.e. without external magnetic field. A maximum critical current density of ~ 3×10^8 A/cm^2 in Y-123 at T = 0 K is predicted from Ginzburg-Landau theory for the de-pairing of Cooper pairs [1]. Various attempts have been undertaken to modify the chemical composition, microstructure and crystallinity of high-temperature superconducting (HTS) thin films in order to increase the values of J_c. Substitution of various rare earth elements for yttrium, ion and neutron irradiation, and substrate pre-treatments are improving the superconducting properties of HTS layers. The incorporation of secondary phase nano-particles into films is a promising concept for enhancing J_c enhancement, since this enables type, density and distribution of such nano-materials to be varied and, consequently, the magnetic flux pinning properties of the films to be optimised. Different types of nano-particles including Ag [2], $BaIrO_3$ [3], $BaSnO_3$ [4], $BaZrO_3$ [5, 6, 7, 8, 9], Y_2BaCuO_5 [10, 11], Y_2O_3 [12, 13, 14] and Y_2O_3-stabilized ZrO_2 [15] have been shown to increase the J_c of Y-123 based composite layers compared to that of phase pure Y-123 films.

Here, we report for the first time the deposition of Y-123 based HTS films from composite $YBa_2Cu_3O_7$ ceramics containing $Y_2Ba_4CuMO_x$ (M-2411, M = Ag, Nb, Ru, Zr) nano-particles. The new phase M-2411 has a double-perovskite cubic structure (lattice parameter a_{2411} = 8.43 Å for Nb-2411) and is chemically very stable with a melting point above 1700 °C [16]. Bulk Y-123 superconductors containing insulating M-2411 nano-particles show strongly enhanced magnetic flux pinning and critical current densities over a range of temperatures and applied magnetic fields [17].

The HTS films in this study were grown on (001) MgO single crystal substrates by pulsed-laser deposition (PLD), with the same deposition parameters employed for all samples [18]. Nano-composite M-2411/Y-123 ceramics were used as targets for the laser ablation process. Ceramics of different composition (M = Ag, Nb, Ru, or Zr) and secondary M-2411 phase content (0 - 15 mol %) were employed. The films are patterned into tracks of width 100 µm and length 1.0 mm by photo-lithography and wet-chemical etching for electrical characterisation by a four point technique. Au/Ag contact pads were evaporated onto the films after in-situ plasma cleaning of their surfaces. The HTS layer thickness as measured by atomic force microscopy (AFM) was ~ 200 nm for all samples if not otherwise stated. X-ray diffraction (XRD, Cu Kα) analysis showed that all layers were epitaxial and oriented parallel to the crystallographic c - axis.

The HTS thin films deposited in this investigation exhibit very different surface morphologies, depending on the ceramic target used for ablation. Figure 1 shows scanning electron micrographs of films produced from Ag-2411 (3 mol %) / Y-123 ceramics (Fig. 1a) and from phase pure Y-123 (0 mol %) ceramics (Fig. 1b). The composite layers are free from micrometer sized

particulates and have a smooth surface with average roughness of 4 – 6 nm (AFM scan range 20 × 20 μm^2). Particulates are present in the pure Y-123 films, however, which exhibit an increased roughness of ~ 10 nm. Ceramics of higher M-2411 content yield films that exhibit particulates of different size, shape and surface density.

All composite layers exhibit metallic resistivity in the normal state with a sharp transition to the superconducting state. Films grown from Ag-2411/Y-123 and Nb-2411/Y-123 ceramics (1 - 3 mol %) have an in-plane resistivity $\rho(300\ K) \approx 0.2\ m\Omega$ cm, which is similar to that observed for Y-123 single crystals ($\rho_{ab} \approx 0.15\ m\Omega$ cm), and critical temperatures $T_{c0} > 88$ K and $T_c^{onset} > 90$ K. By comparison, Y-123 thin films deposited from phase pure ceramics have $T_{c0} \approx 93$ K and $T_c^{onset} \approx 95$ K. Film samples of reduced critical temperatures and higher resistivity are produced from ceramics with higher M-2411 content.

The self-field transport critical current density J_c of HTS layers deposited under identical conditions (laser fluence $\Phi \approx 2.7$ J/cm^2) is summarized in Figure 2. The J_c of films shows a strong and non-monotonic dependence on composition and secondary phase content of the target ceramics. A pronounced maximum of $J_c(77\ K) = 3.4$ MA/cm^2 and 4.2 MA/cm^2 is observed for layers deposited from ceramics containing 2 mol % Ag-2411 and Nb-2411, respectively. Films grown from phase pure Y-123 ceramics have $J_c(77\ K) = 1.05$ MA/cm^2. Ceramics with high secondary phase content do not yield high-quality layers and the critical current densities are ≤ 0.3 MA/cm^2 (Ag-2411 and Nb-2411, 10 - 15 mol %) and < 0.05 MA/cm^2 (Ru-2411 and Zr-2411, 5 – 15 mol %) at 77 K. Multi-layer samples of Y-123//Ag-2411/Y-123//Y-123 were grown by sequential ablation of pure Y-123 and Ag-2411 (10 mol %)/Y-123 ceramics. The number of laser pulses employed was 3000 (Y-123) and 1000 (Ag-2411/Y-123). The amount of secondary phase ablated for such samples was the same as that in the single layer films fabricated from Y-123 ceramics containing 1.43 mol % Ag-2411. The multi-layered samples have enhanced critical current density (2.2 MA/cm^2) and similar values of $T_{c0} = 89$ K and $\rho(300\ K) \approx 0.2\ m\Omega$ cm. Films deposited at higher fluence ($\Phi \approx 3.2$ J/cm^2) from Ag-2411 (2 mol %)/Y-123 ceramics exhibit similar enhancement of J_c, with a highest achieved value $J_c(77\ K) = 5.1$ MA/cm^2. HTS layers deposited on (001) $SrTiO_3$ substrates do not show increased values of J_c using Ag-2411 (2 mol %)/Y-123 ceramic targets compared to pure Y-123. The variation of T_c and J_c of these films is strikingly different to the properties of nano-composite ceramics. The critical temperature $T_{c0} = 91 \pm 0.5$ K for bulk Y-123 superconductors is independent of the secondary phase and the $J_c(77\ K)$ values increase monotonically up to 30 mol % content of Ag-2411 [16].

The composition and crystallinity of the films was investigated by x-ray diffraction analysis (XRD 3 circle system with 2D detector). The XRD intensity distribution in reciprocal space for a thin film sample deposited from Nb-2411 (15 mol %) / Y-123 ceramic is shown in Figure 3a. The

layer thickness of this sample was 400 nm. The diffraction pattern reveals (00ℓ) and (10ℓ) reflections of c-axis oriented Y-123 and the (002) reflection of the MgO substrate. The additional XRD peak marked by circle (Fig. 3a) corresponds to the (220) reflection of Nb-2411. This signal is observed with films deposited from nano-composite ceramic targets and is not detected with phase pure Y-123 films (0 mol % M-2411). The (220) reflection is the most intense diffraction peak of the M-2411 phase [17]. The angular width of the observed (220) Nb-2411 peak, $\Delta(2\theta)_{FWHM}$ = 1.31 °, is larger than that of the (103) Y-123 reflection ($\Delta(2\theta)_{FWHM}$ = 0.81 °). This peak broadening is probably related to size effects and an average Nb-2411 crystallite size of 10 ± 2 nm is estimated from Scherrer's formula. The measured diffraction angles of the (220) peak, 2θ = 30.7 ± 0.7 ° and χ = 43.9 ± 1.6 °, indicate the c-axis orientation and cube-on-cube epitaxy of Nb-2411 crystallites in the Y-123 matrix (calculated angles $2\theta_{th}$ = 30.0 ° and χ_{th} = 45.0 °). This epitaxial structure is confirmed by XRD φ scans of the (103) Y-123 and (220) Nb-2411 reflections (Fig. 3b). Both reflections show maximum intensity at about the same angle φ and a Δφ = 90 ° rotational symmetry (inset of Fig. 3a). The angular width of the Nb-2411 reflection obtained from a fit to the data is $\Delta\varphi_{FWHM}$ = 4.7 °. The lattice mismatch of cubic double-perovskite Nb-2411 (a_{2411} = 8.43 Å) and orthogonal triple-perovskite Y-123 (lattice parameters a_{123} ≅ 3.85 Å and c_{123} = 11.68 Å) is $|(a_{2411} - 2\ a_{123}) / 2\ a_{123}| \approx 9.5$ % and $|(3\ a_{2411} - 2\ c_{123}) / 2\ c_{123}| \approx 8.3$ %. Epitaxial growth of Nb-2411 in Y-123 is observed also in the nano-composite ceramics and the Nb-2411 crystallite size in the bulk materials is ~ 10 - 20 nm [17, 19].

In order to evaluate the formation of the epitaxial Y-123 phase in thin films, XRD ω scans of the (005) Y-123 reflection were performed (so-called rocking curves). From the measured diffraction intensity I(ω) the angular width $\Delta\omega_{FWHM}$ of the rocking curve was determined by fitting a Pseudo-Voigt peak profile to the data. The epitaxial Y-123 phase was quantified by integrating the diffraction intensity over the relevant angle range (epitaxial phase signal $E = \int I(\omega)\, d\omega$). A similar procedure was employed to quantify the epitaxial phase formation in other oxide thin film materials [20]. For c – axis oriented Y-123 films with strong out-of-plane texture the angular widths are typically $\Delta\omega_{FWHM} < 3$ ° depending on the type of substrate, film thickness and XRD apparatus and measurement technique. The thin film samples reported in this study revealed $\Delta\omega_{FWHM}$ = 0.33 ° and $\Delta\omega_{FWHM} \leq 1.2$ ° for the pure Y-123 (0 mol %) and the nano-composite (1 – 3 mol % Ag-2411 and Nb-2411) layers, respectively. The epitaxial phase signal was E = 2.75 and E = 3.09 ± 0.17 (in arbitrary units) for the pure Y-123 and the nano-composite films, respectively. Ceramics of higher M-2411 content (10 and 15 mol %, M = Ag and Nb) yielded layers of reduced crystallinity with E < 2.4 and $\Delta\omega_{FWHM}$ = 0.6 – 3.2 °. The XRD results indicate improved epitaxy of Y-123 on MgO in nano-composite films that are laser-deposited from ceramics of low M-2411 content.

Figure 4 shows the XRD angular width and epitaxial phase signal and the critical current density of various thin films and multi-layers deposited from Ag-2411/Y-123 and Nb-2411/Y-123 nano-composite ceramic targets. Samples revealing enhanced current density $J_c > 2.1$ MA/cm^2 showed moderate angular width $\Delta\omega_{FWHM} \leq 1.2$ ° (Fig. 4a) and strong Y-123 epitaxial signal $E \approx 3$ (Fig. 4b). Such samples were deposited from ceramics containing 1 – 3 mol % M-2411 (thin film samples) and 1.43 mol % Ag-2411 (equivalent content for multi-layer samples) and the corresponding data points are encircled by ellipses in Figure 4. Phase pure Y-123 films had $J_c = 1.05$ MA/cm^2 (triangle symbols, Fig.4). At high M-2411 content (10 and 15 mol %) the films had $J_c < 0.3$ MA/cm^2 and reduced Y-123 phase signals. These results indicate a correlation of J_c of the nano-composite layers with the crystallinity of the Y-123 matrix.

The mechanism of J_c enhancement in the nano-composite films remains to be clarified. The M-2411 nano-particles in films may act as artificial pinning centres. The observed improvement of Y-123 phase formation, the modified layer morphology and the possible stabilization of other phases by the non-equilibrium PLD process may contribute also to the enhancement of J_c in self-field. At 77 K temperature, J_c(2 mol %) / J_c(0 mol %) is 4.0 and 3.2 for Nb-2411/Y-123 and Ag-2411/Y-123, respectively. An enhancement of 3.8×, ≤ 2× and ~ 2× was achieved for $BaZrO_3$, Y_2BaCuO_5 and Y_2O_3 nano-particles in Y-123 [9, 10, 12], respectively. Angle dependent in-field measurements J_c(B) and transmission electron microscopy investigations are under way to investigate the flux pinning behaviour [21] and the defect microstructure of the novel films. The M-2411/Y-123 nano-composite material might also have potential for the fabrication of improved HTS layers on technical substrates.

Acknowledgements

Financial support was received from the Austrian Science Fund FWF (Project P18320), the Austrian Federal Ministry of Economics and Labour (Micro@Nanofabrication Austria network) and the European Science Foundation (Thin Films for Novel Oxide Devices, Nanoscience and Engineering in Superconductivity). K.S. acknowledges support by the Higher Education Commission of Pakistan.

Figure captions

FIGURE 1

Surface micrographs of novel Y-123 based thin films (scanning electron microscopy). Layers deposited from Ag-2411 (3 mol %)/Y-123 nano-composite ceramics reveal smooth surfaces without particulates (a). Films fabricated from single phase Y-123 ceramics contain particulates of micrometer size (b).

FIGURE 2

Self-field critical current density J_c of Y-123 based thin films on (001) MgO. Layers deposited from Ag-2411/Y-123 and Nb-2411/Y-123 ceramics (1 – 3 mol %) show enhanced J_c values in comparison to phase pure Y-123 films (0 mol %). Multi-layered Y-123//Y-123/Ag-2411 //Y-123 samples (ML) also show higher J_c values (diamond symbols).

FIGURE 3

X-ray diffraction (XRD) of films deposited from Nb-2411 (15 mol %)/Y-123 ceramics. The reciprocal space intensity map shows (00ℓ) and (10ℓ) reflections from c-axis oriented Y-123 and the (220) reflection of epitaxial Nb-2411 (marked by circle, a). The (002) MgO substrate peak is indicated by the subscript S. XRD φ scans of (103) Y-123 and (220) Nb-2411 reflections (b). The solid lines represent fits to the data. The reflections show $\Delta\varphi = 90\,^\circ$ rotational symmetry (inset).

FIGURE 4

Self-field critical current density J_c(77 K), XRD angular width $\Delta\omega_{FWHM}$ and epitaxial phase signal E of nano-composite films pulsed-laser deposited from Ag-2411/Y-123 and Nb-2411/Y-123 ceramics. Samples with enhanced $J_c > 2.1$ MA/cm^2 have small widths of the (005) Y-123 reflection, $\Delta\omega_{FWHM} \leq 1.2\,^\circ$ (a), and strong Y-123 signals, $E \approx 3$ (b). Ellipses mark samples produced from ceramics containing 1 – 3 mol % M-2411. Pure Y-123 films (0 mol % M-2411) are marked by triangle symbols). Films deposited from targets with 10 and 15 mol % M-2411 have $J_c < 1$ MA/cm^2 (dashed lines mark J_c value of 1 MA/cm^2).

REFERENCES

[1] TINKHAM M., *Introduction to Superconductivity*, (McGraw-Hill, New York) 1996.

[2] KUMAR D., SHARON M., PINTO R., APTE P.R., PAI S.P., PURANDARE S.C., GUPTA L.C. and VIJAYARAGHAVAN R., *Appl. Phys. Lett.* **62** (1993) 3522.

[3] HÄNISCH J., CAI C., HÜHNE R., SCHULTZ L. and HOLZAPFEL B., *Appl. Phys. Lett.* **86** (2005) 122508.

[4] VARANASI C. V., BARNES P.N., BURKE J., BRUNKE L., MAARTENSE I., HAUGAN T.J., STINZIANNI E.A., DUNN K.A. and HALDAR P., *Supercond. Sci. Technol.* **19** (2006) L37.

[5] MACMANUS-DRISCOLL J.L., FOLTYN S.R., JIA Q.X., WANG H., SERQUIS A., CIVALE L., MAIOROV B., HAWLEY M.E., MALEY M.P. and PETERSON D.E., *Nat. Mater.* **3** (2004) 439.

[6] KANG S., GOYAL A., LI J., GAPUD A.A, MARTIN P.M., HEATHERLY L., THOMPSON J.R., CHRISTEN D.K., LIST F.A., PARANTHAMAN M. and LEE D.F., *Science* **311** (2006) 1911.

[7] WEE S.H., GOYAL A., MARTIN P.M., LI J., PARANTHAMAN M. and HEATHERLY L., *Supercond. Sci. Technol.* **19** (2006) L42.

[8] KANG S., LEONARD K.J., MARTIN P.M., LI J. and GOYAL A., *Supercond. Sci. Technol.* **20** (2007) 11.

[9] GUTIÉRREZ J., LLORDÉS A., GÁZQUES J., GIBERT M., ROMÁ N., RICART S., POMAR A., SANDIUMENGE F., MESTRES N., PUIG T. and OBRADORS X., *Nat. Mater.* **6** (2007) 367.

[10] HAUGAN T., BARNES P.N., WHEELER R., MEISENKOTHEN F. and SUMPTION M., *Nature* **430** (2004) 867.

[11] VARANASI C., BARNES P.N., BURKE J., CARPENTER J. and HAUGAN T.J., *Appl. Phys. Lett.* **87** (2005) 262510.

[12] WANGA H., SERQUIS A., MAIOROV B., CIVALE L., JIA Q.X., ARENDT P.N., FOLTYN S.R., MACMANUS-DRISCOLL J.L. and ZHANG X., *J. Appl. Phys.* **100** (2006) 053904.

[13] CAMPBELL T.A., HAUGAN T.J., MAARTENSE I., MURPHY J., BRUNKE L. and BARNES P., *Physica C* **423** (2005) 1.

[14] MELE P., MATSUMOTO K., HORIDE T., MIURA O., ICHINOSE A., MUKAIDA M., YOSHIDA Y. and HORII S., *Physica C* **445–448** (2006) 648.

[15] MELE P., MATSUMOTO K., HORIDE T., ICHINOSE A., MUKAIDA M., YOSHIDA Y. and HORII S., *Supercond. Sci. Technol.* **20** (2007) 244.

[16] HARI BABU N., IIDA K. and CARDWELL D.A., *Physica C* **445-448** (2006) 353.

[17] HARI BABU N., IIDA K., SHI Y., WITHNELL T.D. and CARDWELL D.A., *Supercond. Sci. Technol.* **19** (2006) S461.

[18] BÄUERLE D., *Laser Processing and Chemistry*, (3rd edition, Springer, Berlin) 2000.

[19] KOBLISCHKA-VENEVA A., KOBLISCHKA M.R., HARI BABU N., CARDWELL D.A. and MÜKLICH F., *Physica C* **445-448** (2006) 379.

[20] PEDARNIG J.D., ROITHER S. and PERUZZI M., *Appl. Phys. Lett.* **89** (2006) 241912.

[21] GUTIÉRREZ J., PUIG T. and OBRADORS X., *Appl. Phys. Lett.* **90** (2007) 162514.

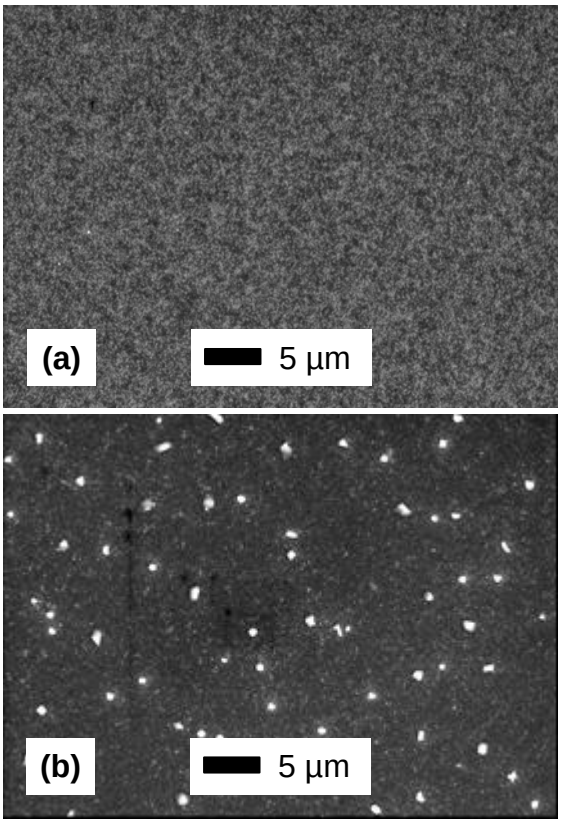
(a)
5 µm
(b)
5 µm

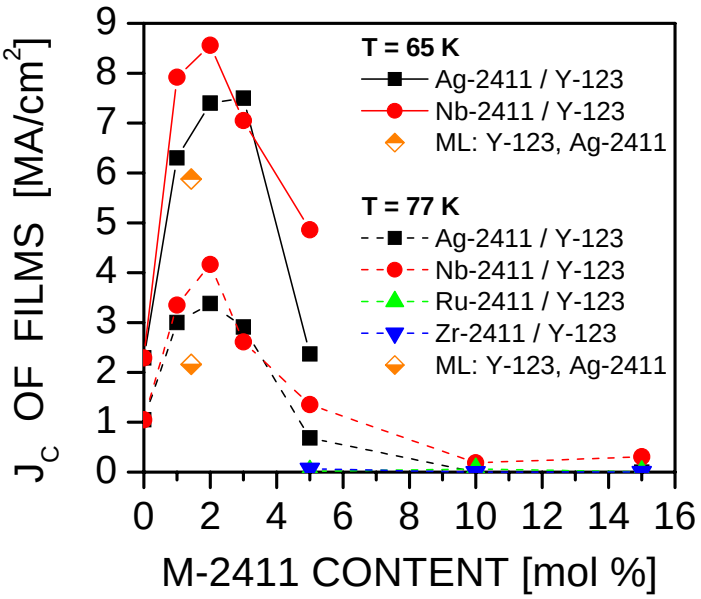
J_c OF FILMS [MA/cm^2]
M-2411 CONTENT [mol %]
T = 65 K
Ag-2411 / Y-123
Nb-2411 / Y-123
ML: Y-123, Ag-2411
T = 77 K
Ag-2411 / Y-123
Nb-2411 / Y-123
Ru-2411 / Y-123
Zr-2411 / Y-123
ML: Y-123, Ag-2411
0
1
2
3
4
5
6
7
8
9
0
2
4
6
8
10
12
14
16

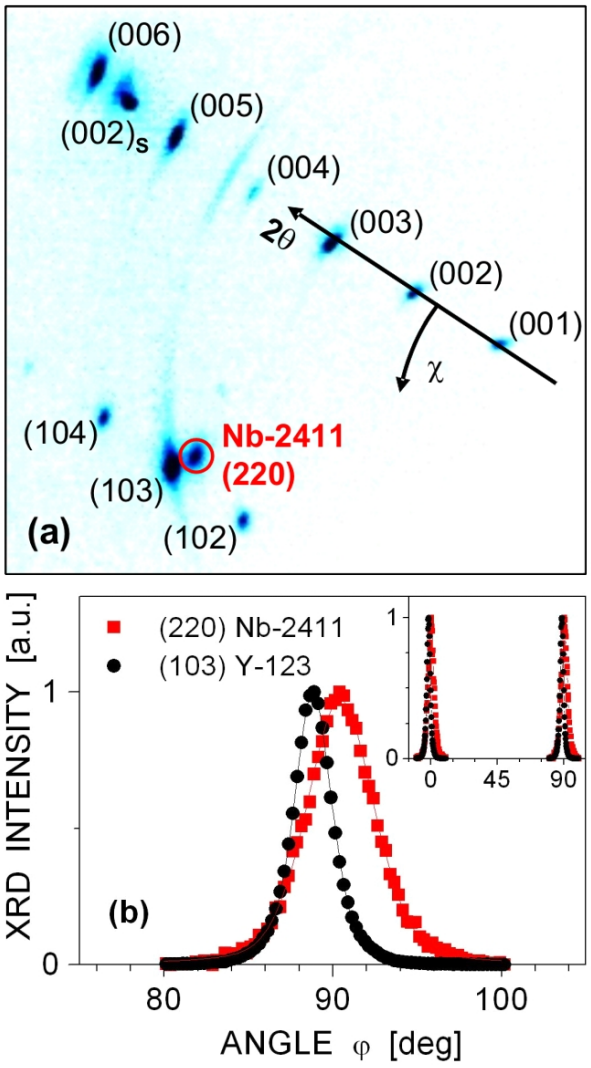
(006)
(005)
(002)s
(004)
2θ
(003)
(002)
(001)
χ
(104)
Nb-2411
(220)
(103)
(a)
(102)
(220) Nb-2411
(103) Y-123
XRD INTENSITY [a.u.]
1
0
80
90
100
ANGLE φ [deg]
(b)
1
0
0
45
90

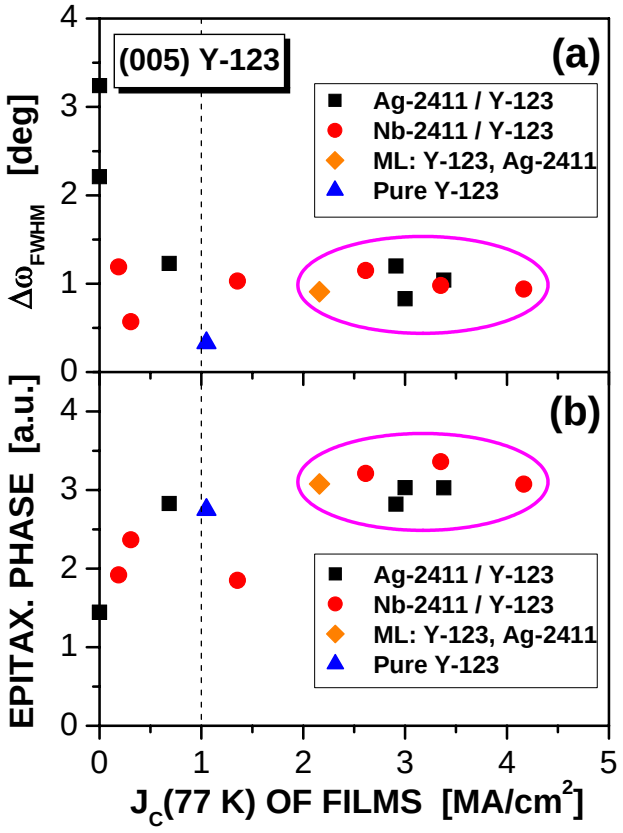
(005) Y-123
(a)
(b)
Ag-2411 / Y-123
Nb-2411 / Y-123
ML: Y-123, Ag-2411
Pure Y-123
Δω_FWHM [deg]
EPITAX. PHASE [a.u.]
J_c(77 K) OF FILMS [MA/cm²]
0
1
2
3
4
5